Available online at www.sciencedirect.com
ScienceDirect
International Journal of Heat and Mass Transfer 50 (2007) 5305–5317
International Journal of HEAT and MASS TRANSFER
www.elsevier.com/locate/ijhmt

# A cubic heat balance integral method for one-dimensional melting of a finite thickness layer

T.G. Myers [a,*], S.L. Mitchell [a], G. Muchatibaya [a], M.Y. Myers [b]

[a] Department of Maths and Applied Maths, University of Cape Town, Rondebosch 7701, South Africa
[b] Department of Molecular and Cell Biology, University of Cape Town, Rondebosch 7701, South Africa

Received 26 February 2007
Available online 3 August 2007

**Abstract**

The work in this paper concerns the one-dimensional melting of a finite thickness layer. An asymptotic series solution describes the temperature in the melt regions. In the solid region the thermal boundary layers are approximated by a cubic polynomial. Results are compared with the exact solution for a semi-infinite block, and shown to agree to within less than 1%. The method is then applied to a situation where no analytical solution is available. A finite thickness frozen solid is placed on a warm substrate in a warm environment: initially the base of the solid heats to the melting temperature when a single melted region develops and subsequently a second melting front appears on the top boundary. We also present an example relevant to heating an ice layer from below, which occurs with de-icing systems.


*Keywords:* Heat balance integral method; Phase change

## 1. Introduction

The melting of a finite block has many interesting natural and industrial applications. Perhaps the most obvious example is the melting of ice in a warm environment, examples in the study of in-flight aircraft and power cable de-icing may be found in [7,12,16,19,21,25]. Melting of ice blocks or ice particles during their transportation for underground refrigeration in mines is described in [24].

If we consider the most simple case of one-dimensional melting then it is possible that there are one, two or three distinct regions during the process, namely a melted layer at the bottom, a solid layer above and another melted layer on the top. The mathematical description then requires solving heat equations in the three regions and coupling these with two Stefan conditions to determine the position of the interfaces. Clearly, there is no general analytical solution and the presence of two moving boundaries, coupled with three partial differential equations, makes the numerical solution problematic. Consequently, the goal of this paper is to determine a relatively simple approximate solution to the problem.

In the following work we focus primarily on ice melting, since data for this problem is easy to acquire. However, the models are applicable to other melting or solidifying systems such as in the metal processing industry. We use two methods to simplify the description of the melting process. In the water region we find that an asymptotic solution, taken to first order, accurately describes the temperature profile. In the ice region the classic boundary layer form of the temperature, particularly for small times, prevents us from using a standard eigenfunction expansion. Instead we modify the heat balance integral method of Goodman and Shea [8,9]. Their method is an adaptation of the Karman–Pohlhausen integral method for analysing boundary layers, see [23]. The approach of Goodman and Shea involved approximating the temperature in the

* Corresponding author. Present address: Division of Applied Mathematics, KAIST, 373-1 Guseong-dong, Yuseong-gu, Daejeon 305-701, Republic of Korea. Tel.: +82 27 21 650 3815; fax: +82 27 21 650 2334.
*E-mail address:* myers@maths.uct.ac.za (T.G. Myers).

0017-9310/$ - see front matter © 2007 Elsevier Ltd. All rights reserved.
doi:10.1016/j.ijheatmasstransfer.2007.06.014

water layer and ice boundary layer by a quadratic polynomial, where the unknown coefficients are chosen to satisfy the boundary conditions and heat equations (the K–P method uses a quartic polynomial). Once melting starts they approximate the temperature throughout the ice by a single quadratic. They also limited their analysis to either fixed temperature or insulated boundary conditions. We adapt this method in a number of significant ways. Firstly, as already mentioned, we use an asymptotic solution in the water. The temperature is described by a power series in odd powers of the co-ordinate. To first order we obtain a cubic. In the case where we can obtain an analytic solution, for example the classical problem of melting an infinite block on a fixed temperature substrate, the small distance or large time expansion of the solution leads to a cubic temperature profile (with no quadratic term), so our series solution has the correct form. This motivates us to also look for a cubic approximation in the ice. Once melting starts the temperature in the ice typically has two boundary layers joined by a region of constant temperature. A single quadratic provides a very poor approximation to this profile, hence we retain two cubics at either side, even after the boundary layers meet. We find that in cases where the quadratic approximation of Goodman and Shea agrees well with an analytical solution then the cubic also shows good agreement, however, we also present a case where the quadratic results in an 11% error for the prediction of the time when melting first occurs. The cubic approximation gives a 0.3% error.

One-dimensional Stefan problems have been studied by a number of authors. The majority of work concentrates on single-phase problems that describes the melting of a solid semi-infinite material, either initially at its melt temperature, or with the assumption that the temperature inside the solid layer prior to melting is constant [11,14,15,27]. The classic self-similarity solution of Neumann is described in Section 3, see [4,10]. The finite thickness block has been investigated in [5,13]. They consider a slab that is insulated on one side while the other side is subjected to a heat input varying arbitrarily with time, with the melted part being removed immediately upon formation. The original partial differential equation is transformed into an ordinary integro-differential equation and solved using successive approximation methods. This method can become very cumbersome if different boundary conditions are used. In addition, the method restricts the initial temperature distribution. More recently, the heat balance integral method has been used both analytically, with a new exponential formulation given in [14], and numerically, as discussed in [2,3] amongst others. Related work has focussed on general numerical models for one-dimensional Stefan problems, including: level set and moving grid methods in [11], a fixed-grid enthalpy formulation in [26], finite volume methods in [22], and explicit variable time-step methods in [28].

In the following section we describe the mathematical problem. In Section 3 we deal with the classical problem of the melting of a semi-infinite block on a fixed temperature substrate. This has an analytical solution which we can then compare with our approximate solution methods. Satisfied that the approximate method is accurate, we move on to the melting of a finite block in a warm environment in Section 4. In this problem the final stage involves solving heat equations in three regions coupled with two Stefan conditions. Finally, we briefly outline the method for modelling a de-icing system, where an energy source at the substrate causes melting.

## 2. Problem description

In this section we describe the governing equations for a finite thickness block of frozen material placed on a warm substrate. We deal only with one-dimensional melting. Energy is supplied by the substrate and also at the free surface and this causes the block to melt. Initially, the block is at a constant temperature $\theta_0$, which is below the melting temperature $\theta_0 < T_m$. Depending on the heat transfer between the block and the surface, melting may occur immediately or there may be an initial transient when the bottom of the block, $z = 0$, heats up to the melting temperature. In either case there will be a growing boundary layer, where heat has diffused into the block, raising its temperature above $\theta_0$. At the top of the block there will also be an exchange of energy between the ambient gas and the block. This will result in a second boundary layer with heat diffusing into (or possibly out of) the block, and may lead to a second melting front. It is possible that the ambient gas removes heat from the block and melting never occurs at the top surface but since the more difficult problem arises with a second melting front, we will focus on that situation. Our main interest is in the thermal problem and so we will neglect the effect of density changes. Of course there is no difficulty in introducing this to the model: for example if the ice and water densities are $\rho_i$ and $\rho_w$ and we have a single water layer of thickness $h$, where the ice block originally has thickness $H$ and the current thickness is $H_c$, then

$$\rho_i(H - H_c) = \rho_w h, \tag{1}$$

provides the appropriate relation between the heights.

In Fig. 1 we depict the four phases that occur when a block is placed on a warm surface in a warm environment which eventually results in two melting fronts. We actually split the problem into four stages. In the first phase, called Phase 1, the block is still below the melting temperature everywhere and there are boundary layers near $z = 0$ and $z = H$. The position of the edge of each boundary layer is denoted $\delta_1$, $\delta_2$ respectively. In Phase 2 melting has commenced at the bottom of the block and so we must deal with a fluid layer there. The temperature at the top is still below the melting temperature. In Phase 2 there is always a region where $\theta = \theta_0$ within the block. Phase 3 begins when the two boundary layers meet, $\delta_1 = \delta_2$, and subsequently the temperature is always above $\theta_0$. Finally Phase 4 commences when the temperature at $z = H$ reaches the melting temperature and a new melting front appears.

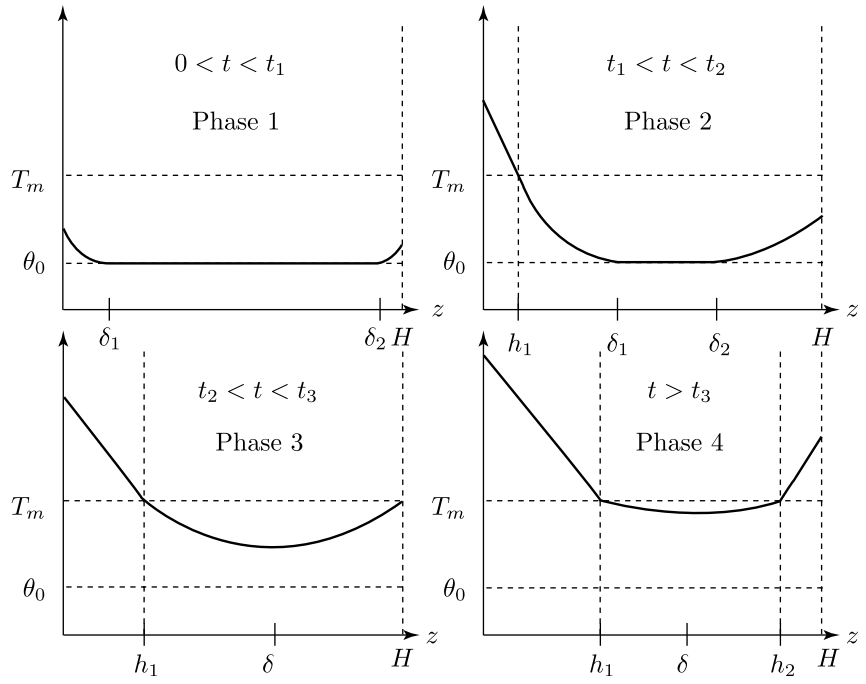


Fig. 1. Schematic of the four phases of melting when a block is placed on a surface above the melting temperature.

Phase 4 can continue until the whole block has melted. The time at which Phase $i$ ends is denoted $t_i$.

It should be noted that the sequence depicted in Fig. 1 is just one possibility. Clearly other sequences are possible. For example if heat is removed at the top surface, such as in aircraft icing, then melting will never occur there. The temperature for $\delta_2 < z < H$ will be below $\theta_0$. Melting may occur at $z = H$ before $\delta_1 = \delta_2$. Also, perfect thermal contact between the block and substrate leads to $\theta(0,t) = T_s$ and melting will occur immediately. However, these variations can all be dealt with by the methods described in the following sections. In particular we will look at the perfect thermal contact problem in Section 3, since this permits an analytical solution and some verification of our analysis.

### 2.1. Governing equations

The most complex version of the problem, occurring in Phase 4, is governed by five equations. These are three heat equations, which describe the temperature in the bottom and top water layers and the ice, and two Stefan conditions, which describe the position of the two melting boundaries. Models for the other phases are special cases of this situation.

The problem is described by the three heat equations

$$\frac{\partial T}{\partial t} = \kappa_w \frac{\partial^2 T}{\partial z^2}, \quad \frac{\partial \theta}{\partial t} = \kappa_i \frac{\partial^2 \theta}{\partial z^2}, \quad \frac{\partial \chi}{\partial t} = \kappa_w \frac{\partial^2 \chi}{\partial z^2}, \tag{2}$$

and two Stefan conditions

$$\rho_i L \frac{dh_1}{dt} = \left( k_i \frac{\partial \theta}{\partial z} - k_w \frac{\partial T}{\partial z} \right)\Big|_{z=h_1}, \quad \rho_i L \frac{dh_2}{dt} = \left( k_i \frac{\partial \theta}{\partial z} - k_w \frac{\partial \chi}{\partial z} \right)\Big|_{z=h_2}, \tag{3}$$

where $T$, $\theta$, $\chi$ represent the temperature in the three layers, $\kappa$ is the thermal diffusivity, $\rho$ the density, $L$ the latent heat of melting and $k$ the conductivity, with subscripts indicating ice or water.

Appropriate boundary conditions are as follows. In the case where the ice layer does not immediately melt at $z = 0$ we apply a Newton cooling condition that includes an energy source term

$$\frac{\partial \theta}{\partial z} = \alpha_1 + \alpha_2(\theta - T_s). \tag{4}$$

A similar condition is imposed at the top surface, $z = H$,

$$\frac{\partial \theta}{\partial z} = \alpha_3 + \alpha_4(T_a - \theta), \tag{5}$$

where $T_s$, $T_a$ denote the substrate and surrounding air temperatures respectively. The source terms $\alpha_1$, $\alpha_3$ can represent a number of effects, such as the energy from an internal heating or cooling system that acts through the substrate. In the ice accretion models described in [1,17–19] supercooled droplets impact on the ice surface. There $\alpha_3$ includes the kinetic energy of incoming water droplets, aerodynamic heating and latent heat of freezing. The sink terms can include convective heat transfer and sublimation for example.

When water appears at $z = 0$ then Eq. (4) is changed to

$$\frac{\partial T}{\partial z} = \alpha_5 + \alpha_6(T - T_s), \tag{6}$$

and when water appears at $z = H$, Eq. (5) is changed to

$$\frac{\partial \chi}{\partial z} = \alpha_7 + \alpha_8(T_a - \chi). \tag{7}$$

Any melting interfaces remain at the melting temperature $T_m$, and so

$$T(h_1,t)=\theta(h_1,t)=T_m,\quad \theta(h_2,t)=\chi(h_2,t)=T_m. \tag{8}$$

Initially the ice temperature is constant. If water appears on $z=0$ at $t=t_1$ and on $z=H$ at $t=t_3$ then

$$\theta(z,0)=\theta_0,\quad h_1(t_1)=h_2(t_3)=0. \tag{9}$$

The system of Eqs. (2), and (3) and corresponding boundary conditions cannot be solved analytically. The presence of the two moving boundaries makes the numerical solution difficult, even in the current one-dimensional problem. Hence we now seek a simplified version of the problem which is amenable to analysis. The route we will follow involves an asymptotic solution in the fluid layers, and a modified version of the heat balance integral method [9] in the ice. We will begin by demonstrating the method on a classical Stefan problem, where a semi-infinite block is placed on a surface that is maintained at constant temperature $T_s > T_m$.

## 3. Melting of a semi-infinite block on a fixed temperature substrate

We now turn to the standard problem where a semi-infinite block is in perfect thermal contact with a substrate of infinite thermal mass. This leads to the two layer problem, with water occupying the region $0<z<h_1(t)$ for $t\geqslant 0$ and ice for $h_1<z$.

The problem is governed by the heat Eq. (2a, b) and the Stefan condition (3a) subject to boundary conditions

$$T(0,t)=T_s,\quad T(h_1,t)=\theta(h_1,t)=T_m,\quad \theta|_{z\to\infty}\to\theta_0, \tag{10}$$

and the two initial conditions

$$\theta(z,0)=\theta_0,\quad h_1(0)=0. \tag{11}$$

This corresponds to the system described in the previous section with no top water layer, $H\to\infty$ and $\alpha_2,\alpha_6\to\infty$ (which then requires $t_1=0$).

The appropriate solution has temperature profiles

$$T=T_s+A\,\mathrm{erf}\frac{z}{2\sqrt{\kappa_w t}},\quad \theta=\theta_0-B\,\mathrm{erfc}\frac{z}{2\sqrt{\kappa_i t}}, \tag{12}$$

and interface height (see [6])

$$h_1(t)=2\lambda\sqrt{\kappa_w t}, \tag{13}$$

where

$$A=\frac{T_m-T_s}{\mathrm{erf}\,\lambda},\quad B=\frac{\theta_0-T_m}{\mathrm{erfc}(\lambda\sqrt{\kappa_w/\kappa_i})},$$

and $\lambda$ is found using the Stefan condition (3a)

$$\rho_i L\sqrt{\pi}\lambda=\frac{k_i}{\sqrt{\kappa_w\kappa_i}}B\mathrm{e}^{-\lambda^2\kappa_w/\kappa_i}-\frac{k_w}{\kappa_w}A\mathrm{e}^{-\lambda^2}. \tag{14}$$

### 3.1. Approximate solution in the water layer

Let us first focus on the water layer and write the problem in non-dimensional form. We set

$$\hat t=\frac{t}{\tau},\quad \hat z=\frac{z}{\mathscr{H}},\quad (\hat T,\hat\theta)=\frac{(T,\theta)-T_m}{\Delta T}, \tag{15}$$

where $\tau$, $\mathscr{H}$ are time and height scales, and the temperature scale is $\Delta T=T_s-T_m$.

The heat equation in the water becomes

$$\frac{\partial\widehat T}{\partial\hat t}=\frac{\tau\kappa_w}{\mathscr{H}^2}\frac{\partial^2\widehat T}{\partial\hat z^2}, \tag{16}$$

and the Stefan condition is now

$$\frac{\rho_i L\mathscr{H}^2}{\tau k_w\Delta T}\frac{\mathrm{d}\hat h_1}{\mathrm{d}\hat t}=\frac{k_i}{k_w}\frac{\partial\hat\theta}{\partial\hat z}-\frac{\partial\hat T}{\partial\hat z}. \tag{17}$$

This determines the time-scale for our melting process, $\tau=\rho_i L\mathscr{H}^2/(k_w\Delta T)$. Substituting this time-scale into the heat equation in the water leads to

$$\frac{\partial^2\widehat T}{\partial\hat z^2}=\frac{k_w\Delta T}{\rho_i L\kappa_w}\frac{\partial\widehat T}{\partial\hat t}=\epsilon\frac{\partial\widehat T}{\partial\hat t}, \tag{18}$$

where $\epsilon=k_w\Delta T/(\rho_i L\kappa_w)$ is independent of the choice of height-scale. Using the parameter values from Table 1 and $\Delta T=20$ °C gives $\epsilon=0.27$.

We now look for a series solution for $\widehat T$ in the form

$$\widehat T=\widehat T_0+\epsilon\widehat T_1+\cdots. \tag{19}$$

The leading and first order equations are

$$\mathscr{O}(\epsilon^0):\frac{\partial^2\widehat T_0}{\partial\hat z^2}=0,\quad \mathscr{O}(\epsilon):\frac{\partial^2\widehat T_1}{\partial\hat z^2}=\frac{\partial\widehat T_0}{\partial\hat t}, \tag{20}$$

with appropriate boundary conditions

$$\widehat T_0=1,\ \widehat T_1=0,\ \text{at }\hat z=0,\quad \widehat T_0=\widehat T_1=0,\ \text{at }\hat z=\hat h_1.$$

To $\mathscr{O}(\epsilon)$ the temperature is then given by

$$\widehat T=1-\frac{\hat z_1}{\hat h_1}-\epsilon\left[\frac{\hat z}{6}\left(1-\frac{\hat z^2}{\hat h_1^2}\right)\right]\frac{\mathrm{d}\hat h_1}{\mathrm{d}\hat t}. \tag{21}$$

In dimensional form this is

$$T=T_s-(T_s-T_m)\frac{z}{h_1}-\frac{T_s-T_m}{6\kappa_w}z\left(1-\frac{z^2}{h_1^2}\right)\frac{\mathrm{d}h_1}{\mathrm{d}t}. \tag{22}$$

The derivative, evaluated at $z=h_1$,

$$\left.\frac{\partial T}{\partial z}\right|_{z=h_1}=-\frac{(T_s-T_m)}{h_1}+\frac{T_s-T_m}{3\kappa_w}\frac{\mathrm{d}h_1}{\mathrm{d}t}, \tag{23}$$

Table 1
Parameter values for ice and water

| | | | | | | | | |
|---|---|---|---|---|---|---|---|---|
| $k_i$ | 2.18 | W/m °C | $k_w$ | 0.57 | W/m °C | $\kappa_i$ | $1.16\times10^{-6}$ | $m^2/s$ |
| $\kappa_w$ | $1.35\times10^{-7}$ | $m^2/s$ | $\rho_i$ | 917 | $kg/m^3$ | $\rho_w$ | 1000 | $kg/m^3$ |
| $T_m$ | 0 | °C | $L$ | $3.34\times10^5$ | J/kg | | | |

will be substituted into the Stefan condition, (3a), once the temperature in the ice is determined.

### 3.2. Approximate solutions in the ice layer

In the ice we employ a modified version of the heat balance integral method of [9]. Goodman and Shea solve melting problems for a finite slab at an initially constant temperature, with two types of boundary condition, namely a fixed temperature substrate $T(0,t) = T_s > T_m$, and a fixed heat flux $\theta_z(0,t) = \alpha_2$. Using the latter boundary condition the first phase of their problem involves determining the temperature in the ice until it reaches the melting temperature. In the ice we expect a thermal boundary layer, of thickness $\delta_1(t)$. The temperature in this boundary layer is approximated by a quadratic polynomial which matches the constant temperature region at $z = \delta_1$. We write the quadratic in terms of $\delta_1(t) - z$, since this simplifies the subsequent algebra

$$\theta(z,t) = a(t) + b(t)(\delta_1(t) - z) + c(t)(\delta_1(t) - z)^2. \tag{24}$$

There are four unknowns $a$, $b$, $c$, $\delta_1$ which are determined as follows. Firstly at $z = 0$ we can apply $\theta_z = \alpha_2$. Further conditions are imposed at the unknown position $\delta_1(t)$, where the temperature smoothly approaches the initial temperature $\theta_0$

$$\theta(\delta_1,t) = \theta_0, \quad \left.\frac{\partial\theta}{\partial z}\right|_{z=\delta_1} = 0.$$

These two conditions lead to $a = \theta_0$, $b = 0$ and the condition at $z = 0$ gives $c = -\alpha_2/2\delta_1$. The temperature can now be expressed in terms of the single unknown $\delta_1$. This is determined by integrating the heat equation between $z = 0$ to $z = \delta_1$, which results in a single first order ODE for $\delta_1$. For $z \geqslant \delta_1$ the temperature is constant, $\theta = \theta_0$. In the case of a finite block a similar analysis may be carried out near the upper surface as long as the two boundary layers do not meet. However, Goodman and Shea neglect the right hand boundary until water appears. The regions may be seen in the diagram for Phase 1 in Fig. 1.

When water appears Goodman and Shea imposed a quadratic temperature profile in the water layer, defined by $z \in [0,h_1]$, and another quadratic all the way across the ice block, $z \in [h_1,H]$. We will use a similar approach but with the following differences. Firstly, the asymptotic solution in the water indicates that the profile is more naturally described by a cubic (with no quadratic term). This is in keeping with the small argument expansion of the error function solutions, (12), in both the ice and water which involve only odd powers of $z$. Consequently we use cubic approximations rather than a quadratic (again in terms of the shifted co-ordinate $\delta(t) - z$). For example in the lower ice boundary layer we set

$$\theta(z,t) = a(t) + b(t)(\delta_1(t) - z) + c(t)(\delta_1(t) - z)^3. \tag{25}$$

The temperature in the water is already in the form of a cubic, given by Eq. (22). Secondly, rather than stretch the single cubic across the whole ice region (which leads to a very poor approximation when water first appears), in Phase 2 we use two cubic profiles to define the two boundary layers in the ice. The two cubics meet when $\delta_1 = \delta_2$, as shown in Fig. 1.

However, for the current problem we are only interested in the behaviour near $z = h_1$ to compare with the error function solution. In this case the method proceeds as follows. Choosing (25) to represent the temperature profiles for $z \in [h_1,\delta_1]$ and imposing the boundary conditions at $z = \delta_1$ we find, as with the quadratic case, that $a = \theta_0$, $b = 0$. The interface condition $\theta(h_1,t) = T_m$ gives

$$c(t) = \frac{T_m - \theta_0}{(\delta_1 - h_1)^3}.$$

We define the integral of the temperature as

$$\tilde{\theta}(t) = \int_{h_1}^{\delta_1} \theta \,\mathrm{d}z = (\delta_1 - h_1)\frac{3\theta_0 + T_m}{4}.$$

Integrating the heat equation in the ice from $z = h_1$ to $z = \delta_1$ gives

$$\kappa_i\left[\left.\frac{\partial\theta}{\partial z}\right|_{z=\delta_1} - \left.\frac{\partial\theta}{\partial z}\right|_{z=h_1}\right] = \int_{h_1}^{\delta_1}\frac{\partial\theta}{\partial t}\mathrm{d}z = \frac{\mathrm{d}\tilde{\theta}}{\mathrm{d}t} - \theta_0\frac{\mathrm{d}\delta_1}{\mathrm{d}t} + T_m\frac{\mathrm{d}h_1}{\mathrm{d}t}, \tag{26}$$

where we have taken the time derivative outside the integral. Substituting for $\theta_z$ and $\tilde{\theta}$ leads to the following equation for $\delta_1$, $h_1$:

$$\frac{12\kappa_i}{\delta_1 - h_1} = \frac{\mathrm{d}\delta_1}{\mathrm{d}t} + 3\frac{\mathrm{d}h_1}{\mathrm{d}t}. \tag{27}$$

A second equation comes from substituting for $\theta_z$ and $T_z$ (given by Eq. (23)) into the Stefan condition (3a)

$$\left[\rho_i L - \frac{k_w(T_m - T_s)}{3\kappa_w}\right]\frac{\mathrm{d}h_1}{\mathrm{d}t} = -3k_i\frac{T_m - \theta_0}{\delta_1 - h_1} - k_w\frac{T_m - T_s}{h_1}. \tag{28}$$

The original problem, defined in terms of two PDEs for the temperature and an ODE for the interface position, has now been reduced to two first order, coupled ODEs for $\delta_1$ and $h_1$.

### 3.3. Comparison of results

The physical parameter values used in this and following sections are given in Table 1. We also impose the $\alpha_i$ values from Table 2 in the boundary conditions. The two values $\alpha_1$, $\alpha_4$ were chosen based on some simple experiments. Ice sheets formed in a freezer at −20 °C were placed on a large piece of metal (W400 steel) in a walk-in incubator, at 31 °C.

Table 2
Parameter values used in Section 3 and 4

| | | | | | | | | |
|---|---|---|---|---|---|---|---|---|
| $H$ | 0.05 | m | $T_a$ | 31 | °C | $\theta_0$ | −20 | °C |
| $T_m$ | 0 | °C | $T_s$ | 31 | °C | $\alpha_2$ | 350 | $m^{-1}$ |
| $\alpha_4$ | 10 | $m^{-1}$ | $\alpha_6$ | 1500 | $m^{-1}$ | $\alpha_8$ | 200 | $m^{-1}$ |

The time taken for the bottom and top surfaces to start melting was measured. Melting at the bottom occurred almost immediately, hence we choose $\alpha_1$ to give initial melting around 1 s. The parameter $\alpha_4$ was chosen to match the time when the top of the block started to melt, and $\alpha_6$, $\alpha_8$ are typical values taken from published literature. $\alpha_1$, $\alpha_4$, $\alpha_6$, $\alpha_8$ correspond to heat transfer coefficients between the ice and substrate, ice and air, water and substrate and water and air of 763, 21.8, 855, 114 W m$^{-2}$ respectively. Any $\alpha_i$ not quoted in Table 2 is set to zero.

In Fig. 2 we compare temperature profiles, at times $t = 1$, 5, 10, 20 s, obtained via the approximate and exact methods. The dashed line on the figures is the exact solution for the temperatures in the two regions, and the solid line is the approximate solution. Within the water layer there is no visible difference, whereas within the ice layer there is a slight difference which is most noticeable near $z = \delta_1$ (marked with a '*'). However, the important point is that the gradients near $z = h_1$ are similar since it is the temperature gradient that determines $h_1$. In this example, the error in $h_1$ remains constant, around 1.3%.

We do not show the result of the quadratic approximation in Fig. 2 since that curve is very close to the two already shown and therefore makes it difficult to distinguish them. In this example the quadratic approximation gives a slightly better agreement for $h_1$. However, in Phase 1 described in the following section, we can also obtain an analytical solution where we find that the time at which water first appears is predicted to within 0.3% by the cubic approximation, but only within 11% by the quadratic. Consequently we prefer the cubic approximation because it provided accurate results in all our tests, is consistent with the asymptotic approximation in the water and the small argument expansion of the error functions, and finally the quadratic solution has a discontinuity in the gradient where the temperature reaches $\theta_0$. The quadratic gives $\theta_{zz}(\delta_1, t) = 2\,c(t)$, the cubic joins smoothly to the flat region, $\theta_{zz}(\delta_1, t) = 0$.

In [14] a similar one-dimensional problem is investigated. They use an exponential approximating function, motivated by the fact that $\mathrm{erf}(z) \sim z\mathrm{e}^{-z^2}$. Using this approximation for the problem of this section gives a prediction of $h_1$ which is very similar to the cubic approximation. However, when applied to Phase 1 of the next section, the results are significantly worse: the time at which water first appears is predicted to within only 23%, rather than 0.3% for the cubic.

## 4. Melting in a warm environment

We now move on to a general problem for which there is no analytical solution. Furthermore, since the final state involves two moving boundaries and heat equations in three regions, the numerical solution is also complicated. As discussed in Section 1, the melting of a finite block may occur in four distinct phases, we will work through each one separately.

**Phase 1.** In this initial phase a block with constant temperature $\theta_0 < T_m$ is placed on a warm surface. The block heats up at the bottom due to the heat transfer between the surface and the block. At the top of the block

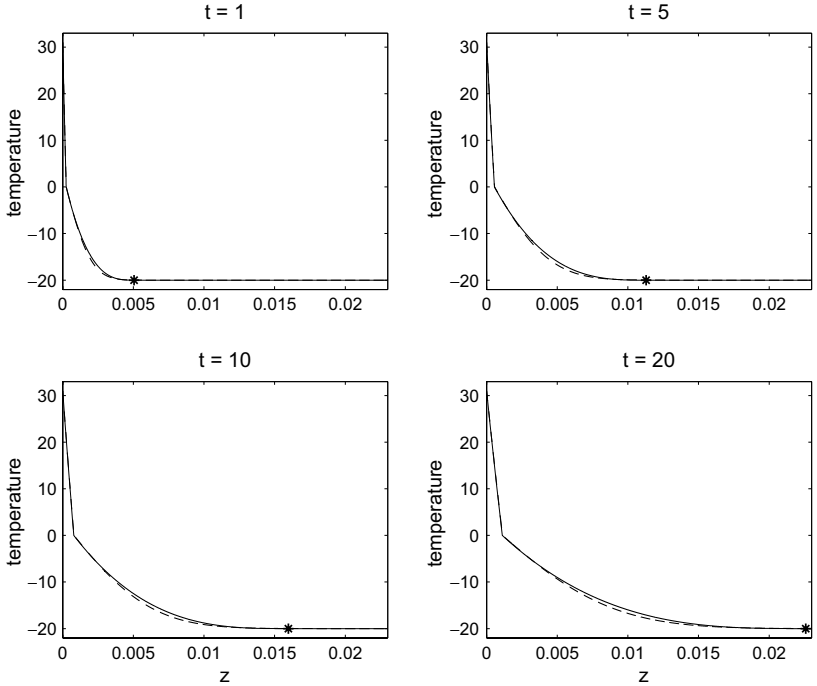


Fig. 2. Comparison of the exact error function solution (dashed line) with the approximate cubic solution (solid line) at $t = 1$, 5, 10, 20 s, '*' denotes the position of $\delta_1$.

there will also be an increase in temperature due to contact with the ambient gas, which we assume to be at a temperature $T_a > T_m$. The end of this phase arises when melting begins at $z = 0$, we denote the time this occurs as $t = t_1$.

For $0 < t < t_1$ we solve the heat equation (2b) in the ice boundary layers, $z \in [0, \delta_1]$, $z \in [\delta_2, H]$. In between we set $\theta = \theta_0$ for $\delta_1(t) < z < \delta_2(t)$. Note that since this phase occurs for a short time we never allow $t$ to be large enough so that $\delta_1 = \delta_2$. We use boundary conditions (4) and (5) at $z = 0$ and $z = H$ respectively. At the edges of the boundary layers $z = \delta_1$, $\delta_2$ we impose the continuity conditions

$$\theta = \theta_0, \quad \frac{\partial \theta}{\partial z} = 0, \quad \text{at } z = \delta_1(t), \delta_2(t). \tag{29}$$

Finally, we close the system with the single initial condition $\theta(z, 0) = \theta_0$.

If we denote the temperature in the two boundary layers as $\theta = \theta_1$ for $z \in [0, \delta_1]$ and $\theta = \theta_2$ for $z \in [\delta_2, H]$ then the cubic approximations become

$$\theta_1(z,t) = \theta_0 - \frac{\alpha_1 + \alpha_2(\theta_0 - T_s)}{\delta_1(t)^2(3 + \alpha_2\delta_1(t))}(\delta_1(t) - z)^3, \tag{30}$$

$$\theta_2(z,t) = \theta_0 - \frac{\alpha_3 + \alpha_4(T_a - \theta_0)}{(H - \delta_2(t))^2(3 + \alpha_4(H - \delta_2(t)))} \times (\delta_2(t) - z)^3. \tag{31}$$

Integrating the heat equation for $z \in [0, \delta_1]$ leads to an equation for $\delta_1$, namely

$$\frac{\mathrm{d}}{\mathrm{d}t}\left[\frac{\delta_1(t)^2}{3 + \alpha_2\delta_1(t)}\right] = \frac{12\kappa_i}{3 + \alpha_2\delta_1(t)}, \quad \delta_1(0) = 0. \tag{32}$$

This has the implicit solution

$$\frac{1}{2}\alpha_2^2\delta_1(t)^2 + 3\alpha_2\delta_1(t) - 9\ln[3 + \alpha_2\delta_1(t)] = 12\kappa_i\alpha_2^2 t - 9\ln 3. \tag{33}$$

For $\delta_2(t) < z < H$, a similar calculation gives

$$\frac{\mathrm{d}}{\mathrm{d}t}\left[\frac{(H - \delta_2(t))^2}{3 + \alpha_4(H - \delta_2(t))}\right] = \frac{12\kappa_i}{3 + \alpha_4(H - \delta_2(t))}, \quad \delta_2(0) = H. \tag{34}$$

This has an implicit solution of the same form as (33) but with $\alpha_2$ replaced by $\alpha_4$ and $\delta_1$ replaced by $H - \delta_2$.

Phase 1 ends when the bottom of the ice reaches the melting temperature $\theta_1(0, t_1) = T_m$, substituting this into (30) gives the boundary layer thickness when this occurs

$$\delta_1(t_1) = \frac{3(\theta_0 - T_m)}{\alpha_1 + \alpha_2(T_m - T_s)}. \tag{35}$$

The corresponding time $t_1$ may be calculated from (33).

For this stage of the problem we can obtain analytical solutions by noting that the boundary layer is small compared to the block thickness and so we can replace the boundary conditions at $\delta_1$, $\delta_2$ by

$$\left.\frac{\partial \theta_1}{\partial z}\right|_{z\to\infty} = 0, \quad \left.\frac{\partial \theta_2}{\partial z}\right|_{z\to-\infty} = 0.$$

This leads to

$$\theta_1(z,t) = \theta_0 - \frac{\alpha_1 + \alpha_2(\theta_0 - T_s)}{\alpha_2}\left[\operatorname{erfc}\left(\frac{z}{2\sqrt{\kappa_i t}}\right) - \mathrm{e}^{\alpha_2 z + \kappa_i t\alpha_2^2} \times \operatorname{erfc}\left(\frac{z}{2\sqrt{\kappa_i t}} + \alpha_2\sqrt{\kappa_i t}\right)\right], \tag{36}$$

$$\theta_2(z,t) = \theta_0 + \frac{\alpha_3 + \alpha_4(T_a - \theta_0)}{\alpha_4}\left[\operatorname{erfc}\left(\frac{H - z}{2\sqrt{\kappa_i t}}\right) - \mathrm{e}^{\alpha_4(H-z) + \kappa_i t\alpha_4^2} \times \operatorname{erfc}\left(\frac{H - z}{2\sqrt{\kappa_i t}} + \alpha_4\sqrt{\kappa_i t}\right)\right]. \tag{37}$$

The exact and approximate solutions are shown in Fig. 3 at time $t \approx 1.87$ s, with the parameter values given in Tables 1 and 2. At this time the temperature at $z = 0$ has just reached 0 °C and so this marks the end of Phase 1. The positions $\delta_1$, $\delta_2$ are marked with '*'s. In the region $z \leqslant \delta_1$ a slight difference in the two solutions can be observed, particularly near $z = \delta_1$. The curves near $z = H$ are virtually identical. In this example melting starts when $t_1 = 1.8704$ s according to the exact solution and at $t_1 \approx 1.8765$ s according to the cubic approximation (which represents a 0.3% difference). The quadratic approximation gives $t_1 \approx 1.6682$ s, representing an 11% difference, and the exponential approximation (similar to that considered in [14]) gives $t_1 \approx 1.4491$ s representing a 23% difference. Therefore, as discussed in the previous section, the cubic profile gives better agreement to the exact solution and we do not consider the quadratic or exponential profiles further.

**Phase 2.** This phase begins when the bottom surface starts to melt and ends when the two boundary layers meet, $\delta_1 = \delta_2$. The initial values of $\delta_1$ and $\delta_2$ are simply those determined at the end of the previous phase. With the

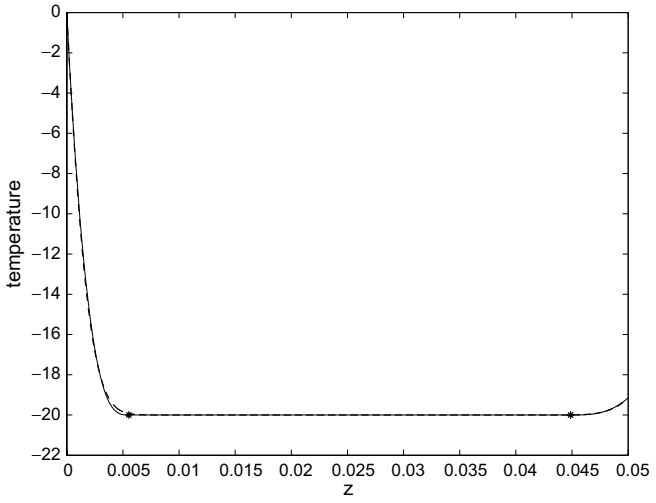


Fig. 3. Temperature profile at the end of Phase 1 when $t = t_1 \approx 1.87$ s. The dashed line denotes the exact solution and the solid line denotes the cubic approximation, '*'s denote the positions $\delta_1$ and $\delta_2$.

appearance of a water layer, we introduce the temperature $T$ and the interface position $h_1$, where $h_1(t_1) = 0$.

The calculation at the top of the block remains unchanged. At $z = 0$ we now impose (6) and at $z = h_1$ Eq. (8a) holds.

Using the method described in Section 3.1 we find the temperature in the water to be

$$T(z,t) = T_m + \frac{\beta_1}{1+\alpha_6 h_1}(z-h_1) - \frac{\beta_1}{6\kappa_w(1+\alpha_6 h_1)^2}\left[3\left(z^2 - \frac{h_1^2(1+\alpha_6 z)}{1+\alpha_6 h_1}\right) + \alpha_6\left(z^3 - \frac{h_1^3(1+\alpha_6 z)}{1+\alpha_6 h_1}\right)\right]\frac{dh_1}{dt}, \quad (38)$$

where, for convenience, we write $\beta_1 = \alpha_5 + \alpha_6(T_m - T_s)$. The temperature gradient at the interface is

$$\left.\frac{\partial T}{\partial z}\right|_{z=h_1} = \frac{\beta_1}{1+\alpha_6 h_1} - \frac{\beta_1 h_1}{3\kappa_w(1+\alpha_6 h_1)^3}[3+3\alpha_6 h_1 + \alpha_6^2 h_1^2]\frac{dh_1}{dt}. \quad (39)$$

In the ice boundary layer, $z \in [h_1, \delta_1]$, the temperature profile is

$$\theta_1(z,t) = \theta_0 + \frac{T_m - \theta_0}{(\delta_1 - h_1)^3}(\delta_1 - z)^3. \quad (40)$$

Integrating the heat equation in the ice between $[h_1, \delta_1]$ and applying (40) gives a first order ODE involving $h_1$, $\delta_1$. The Stefan condition provides a second relation and so in the lower region the process is described by

$$[\rho_i L - k_w f(h_1)]\frac{dh_1}{dt} = \frac{3k_i(\theta_0 - T_m)}{\delta_1 - h_1} - \frac{k_w \beta_1}{1+\alpha_6 h_1}, \quad (41)$$

$$3\frac{dh_1}{dt} + \frac{d\delta_1}{dt} = \frac{12\kappa_i}{\delta_1 - h_1}, \quad (42)$$

where

$$f(h_1) = \frac{\beta_1 h_1}{3\kappa_w(1+\alpha_6 h_1)^3}[3+3\alpha_6 h_1 + \alpha_6^2 h_1^2]. \quad (43)$$

Note that Eqs. (41) and (42) are independent of $\delta_2$. However, we still need to calculate the temperature in the upper region to determine the end of phase 2. This could occur because either $\delta_1 = \delta_2$ or the top starts to melt, $\theta_2(H,t) = T_m$. We choose the first condition now and deal with the second in Phase 4. In the ice accretion model used in [17–20] it is assumed that the layers are sufficiently thin that a linear approximation holds. The contribution of the water layer in that model is represented by the final term in (41). The difference obtained by taking the cubic approximation, i.e. including the next term in the series expansion, introduces the correction factor $+k_w f(h_1)\frac{dh_1}{dt}$. Since the correction term simply moves to the left hand side of (41), the final calculation is just as simple as in the linear approximation but there is a distinguishable gain in accuracy.

In the ice for $z \in [\delta_2, H]$, Eq. (31) describes the temperature. Eq. (34) determines $\delta_2$ and so we solve this simultaneously with (41) and (42) to find the end of Phase 2 and hence a new calculation must begin. We denote the time that Phase 2 ends as $t_2$.

**Phase 3.** This phase begins when the boundary layers meet, $\delta_1 = \delta_2$ at $t = t_2$, it ends when the top layer reaches the melting temperature, $\theta(H,t) = T_m$ at $t = t_3$, and we must then start a calculation with a second water layer.

Since there has been no change to the model in the water layer the temperature for $z \in [0, h_1]$ is still defined by Eq. (38). During Phase 2 we approximated the temperature at either side of the block by two cubics. Obviously we would now hope to simplify the analysis by applying a single cubic across the whole layer; Goodman and Shea use a single quadratic as soon as melting starts at $z = 0$. Unfortunately, the solution profile still has a very shallow base and steep edges, so a single quadratic or cubic polynomial does not provide a good fit. We therefore use two cubic profiles which meet at the point $z = \delta(t)$ with the initial condition $\delta(t_2) = \delta_1(t_2) = \delta_2(t_2)$. Our previous functions $\delta_1$, $\delta_2$ defined the points where the temperature reached $\theta_0$ and $\theta_z = 0$. Once the boundary layers meet then the temperature will rise above $\theta_0$ but there will still be a point where the temperature gradient is zero. This provides our definition of $\delta$, namely

$$\theta_1(\delta) = \theta_2(\delta), \quad \left.\frac{\partial \theta_1}{\partial z}\right|_{z=\delta} = \left.\frac{\partial \theta_2}{\partial z}\right|_{z=\delta} = 0.$$

The temperature for $z \in [h_1, \delta]$, $z \in [\delta, H]$ is now given by

$$\theta_1(z,t) = \theta_{mn}(t) + \frac{T_m - \theta_{mn}(t)}{(\delta(t) - h_1)^3}(\delta(t) - z)^3 \quad \text{for } h_1 \leqslant z \leqslant \delta, \quad (44)$$

$$\theta_2(z,t) = \theta_{mn}(t) - \frac{\alpha_3 + \alpha_4(T_a - \theta_{mn}(t))}{(H - \delta(t))^2(3 + \alpha_4(H - \delta(t)))}(\delta(t) - z)^3 \quad \text{for } \delta \leqslant z \leqslant H. \quad (45)$$

We no longer need to find two boundary layer thicknesses but, since we no longer know the minimum temperature in the block, we have introduced a new unknown $\theta_{mn}(t)$ which, in this case, is an increasing function of time. Substituting the temperature expressions into the heat equation and integrating over $(h_1, \delta)$ and $(\delta, H)$ leads to two ODEs

$$\frac{3\kappa_i(T_m - \theta_{mn})}{\delta - h_1} = \frac{d}{dt}\left[(\delta - h_1)\frac{(T_m + 3\theta_{mn})}{4}\right] + T_m\frac{dh_1}{dt} - \theta_{mn}\frac{d\delta}{dt}, \quad (46)$$

$$\frac{3\kappa_i(\alpha_3 + \alpha_4(T_a - \theta_{mn}))}{3 + \alpha_4(H - \delta)} = \frac{d}{dt}\left[\theta_{mn}(H - \delta) + \frac{1}{4}\frac{(\alpha_3 + \alpha_4(T_a - \theta_{mn}))}{3 + \alpha_4(H - \delta)}(H - \delta)^2\right]b + \theta_{mn}\frac{d\delta}{dt}. \quad (47)$$

These equations involve three unknowns, $\theta_{mn}(t)$, $\delta(t)$, $h_1(t)$, and the system is closed by the addition of the Stefan condition (41), with $\theta_0$ replaced by $\theta_{mn}(t)$, the three initial conditions for $h_1(t_2)$, $\delta(t_2)$ (determined from the previous phase) and $\theta_{mn}(t_2) = \theta_0$.

Hence this phase is described by three nonlinear first order ODEs. It ends at time $t = t_3$, when $\theta(H,t) = T_m$, which is found from the relation

$$T_m = \theta_{mn}(t_3) - \frac{\alpha_3 + \alpha_4(T_a - \theta_{mn}(t_3))}{3 + \alpha_4(H - \delta(t_3))}(\delta(t_3) - H). \tag{48}$$

**Phase 4.** In this final phase both surfaces of the block melt and so we have two water layers and two moving fronts, denoted by $h_1$, $h_2$. This phase will continue until the block has completely melted, when $h_1 = h_2$.

The temperature in the lower water layer $\theta_1(z,t)$ is still specified by Eq. (38). In the solid the temperature between $h_1$, $\delta$ remains unchanged from the previous section, (44). In the region $z \in [\delta, h_2]$ the new boundary condition $\theta_2(h_2,t) = T_m$ results in the profile

$$\theta_2 = \theta_{mn} + \frac{T_m - \theta_{mn}}{(\delta - h_2)^3}(\delta - z)^3. \tag{49}$$

In the new water layer, the temperature is governed by the heat Eq. (2c) subject to the cooling condition (7) and $\chi(h_2,t) = T_m$. Following the same method as for the lower water layer we find

$$\chi(z,t) = T_m + \frac{\beta_2}{1 + \alpha_8(H - h_2)}(z - h_2) - \frac{\beta_2}{6\kappa_w(1 + \alpha_8(H - h_2))^2}\left[(H - z)^2(3 + \alpha_8(H - z)) - \frac{(H - h_2)^2(1 + \alpha_8(H - z))}{1 + \alpha_8(H - h_2)}(3 + \alpha_8(H - h_2))\right]\frac{dh_2}{dt}, \tag{50}$$

where $\beta_2 = \alpha_7 + \alpha_8(T_a - T_m)$. The temperature gradient required in the Stefan condition is

$$\left.\frac{\partial\chi}{\partial z}\right|_{z=h_2} = \frac{\beta_2}{1 + \alpha_8(H - h_2)} + \frac{\beta_2(H - h_2)}{3\kappa_w(1 + \alpha_8(H - h_2))^3} \times [3 + 3\alpha_8(H - h_2) + \alpha_8^2(H - h_2)^2]\frac{dh_2}{dt}. \tag{51}$$

At this stage we can proceed as before, integrating the heat equation in the ice layer between $[h_1, \delta_1]$ and $[\delta_2, h_2]$ to find two differential equations. The Stefan conditions at the two water interfaces then provide another two ODEs and we are left with a system of four equations for the unknowns $\theta_{mn}$, $\delta$, $h_1$, $h_2$.

As the phases have progressed the complexity of the model has increased, due to the increasing number of regions and moving boundaries. In Phase 4 we have four unknowns, however, we can make a significant simplification by noting that the temperature in the ice is close to zero everywhere and the temperature gradient in the ice is much less than that in the water layers. If we neglect the contribution of the ice to the evolution of $h_1$, $h_2$ then the problem is governed by

$$[\rho_i L - k_w f(h_1)]\frac{dh_1}{dt} = -\frac{k_w\beta_1}{1 + \alpha_6 h_1},$$
$$[\rho_i L + k_w g(h_2)]\frac{dh_2}{dt} = -\frac{k_w\beta_2}{1 + \alpha_8(H - h_2)}, \tag{52}$$

where

$$g(h_2) = \frac{k_w\beta_2(H - h_2)}{3\kappa_w(1 + \alpha_8(H - h_2))^3}[3 + 3\alpha_8(H - h_2) + \alpha_8^2(H - h_2)^2], \tag{53}$$

and $f(h_1)$ is defined in (43). We therefore only have to solve two ODEs for two unknowns. As usual the initial condition on $h_1$ comes from the previous phase, we also impose $h_2(t_3) = H$.

### 4.1. Results

In Fig. 3 we show the temperature profile at the end of Phase 1 with the parameter values given in Tables 1 and 2. In Figs. 4–8 we show results for the subsequent stages.

Fig. 4 shows the temperature profile at $t \approx 32.59$ s, and this marks the end of Phase 2. The two boundary layers meet at $z = \delta = 0.0285$ m, which is marked by a '*'. The water height at this time is $h_1 \approx 8.2 \times 10^{-4}$ m. At this stage it is still possible to obtain an analytical solution in the top region. This is shown as the dotted line, which agrees almost exactly with the approximate solution for $z \in [\delta, H]$.

After the boundary layers meet the energy from the lower layer affects the temperature in the upper region and the error function solution becomes invalid. This may be seen in Fig. 5, which shows a temperature profile

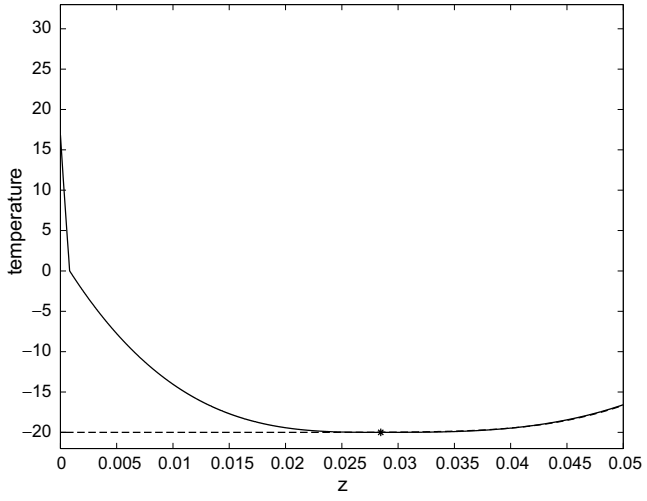


Fig. 4. Temperature profile at the end of Phase 2 when $t_2 \approx 32.59$ s and $\delta_1 = \delta_2 \approx 0.0285$ m (denoted here by '*'). The dashed line denotes the exact solution near the right boundary, Eq. (37).

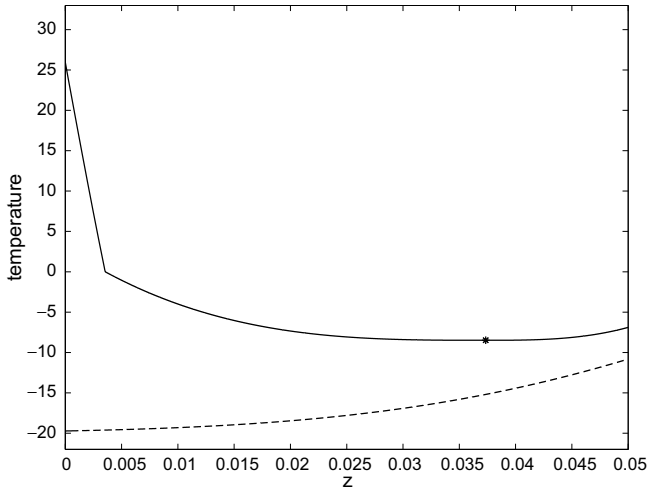


Fig. 5. Temperature profile during Phase 3, at $t = 300$ s, where '*' denotes the position of $\delta \approx 0.037$ m. The dashed line denotes the exact solution near the right boundary, Eq. (37).

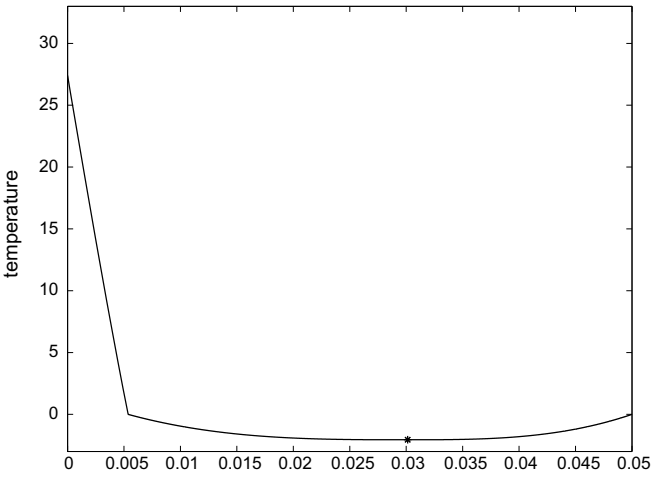


Fig. 6. Temperature profile at the end of Phase 3 when $t_3 \approx 561.61$ s, $\delta \approx 0.03$ m and $\theta(H,t) = T_m$.

in Phase 3, at $t = 300$ s, where the temperature is everywhere greater than that predicted by the analytical solution. The height of the water layer, $h_1 \approx 3.46 \times 10^{-3}$ m, is significantly greater than in Fig. 4; also the position $z = \delta \approx 0.0373$ m, marked by a '*', has moved to the right.

Phase 3 ends when $t = t_3 \approx 561.61$ s; this is shown in Fig. 6. At this stage $\delta \approx 0.03$ m has moved back towards the centre and $h_1 \approx 5.4 \times 10^{-3}$ m. As mentioned at the end of the previous section, the temperature gradient in the ice is small at this time, and becomes smaller as time increases. This is the motivation for neglecting the effect of the ice layer on the evolution of the interfaces during Phase 4.

Fig. 7 shows a temperature profile during Phase 4, at $t = 700$ s (which is well into Phase 4). We have plotted two sets of profiles, the solid line is a product of the full calculation, including the ice layer temperature. For the dashed line we set $\theta = 0$ and solve (52) for the water layer

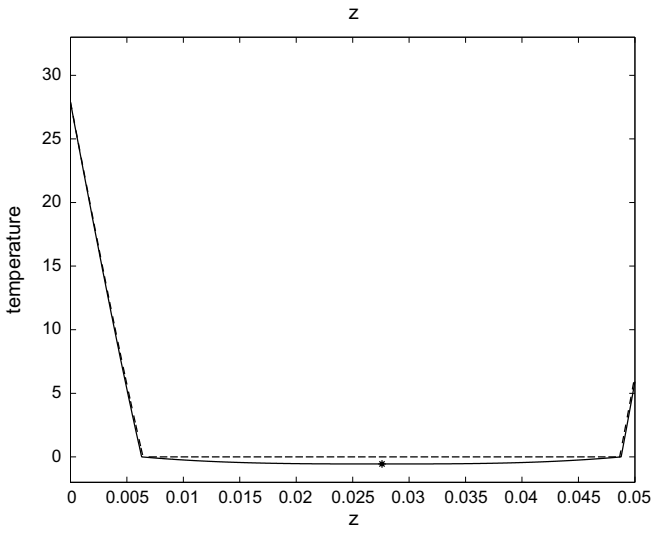


Fig. 7. Temperature profile during Phase 4, at $t = 700$ s. The solid line includes the ice layer, and $\delta$ is marked by a '*', and the dashed line neglects the ice layer.

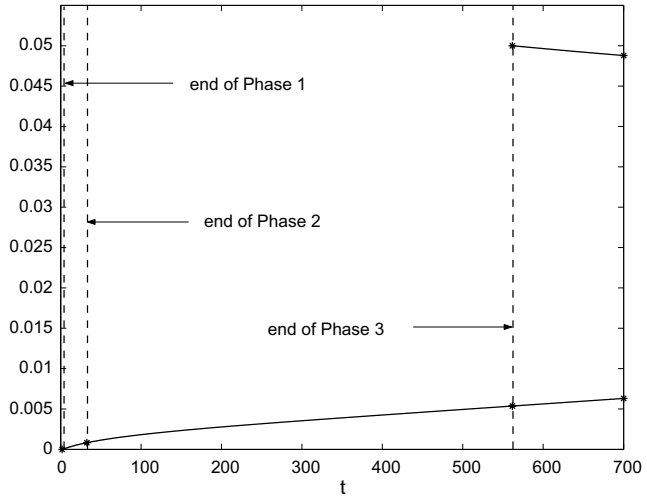


Fig. 8. Development of $h_1$ (lower line) and $h_2$ (upper line), with $t_1, t_2, t_3 \approx 1.87, 32.6, 561.6$ s.

thicknesses. Within the ice the temperature difference is obvious, however the temperature in the water is hardly effected by this approximation. For the full calculation we find $h_1 \approx 6.3 \times 10^{-3}$ m, $h_2 \approx 4.87 \times 10^{-2}$ m at $t = 700$ s. Neglecting the ice layer we find $h_1 \approx 6.4 \times 10^{-3}$ m, $h_2 \approx 4.865 \times 10^{-2}$ m (i.e. errors of 2% and 0.2% respectively). Since the boundary conditions on the ice layer are now symmetric, $\theta = T_m$ at $z = h_1, h_2$, the position of $\delta$ must move towards the centre of the ice layer and eventually remain at this point. This is confirmed in Fig. 7 where the full calculation gives $\delta = 0.0276$ m and $\frac{1}{2}(h_1 + h_2) = 0.0275$ m.

Finally, in Fig. 8 we show the development of the water layers. The vertical dashed lines show the position of each phase. Initially there is no water, $h_1 = h_2 = 0$, after 1.87 s water appears at $z = 0$. After 32.6 s the ice boundary layers

meet, signifying the end of Phase 2. Phase 3 starts when water appears at $z = H$ at $t_3 = 561.6$ s. The calculation may then be continued until $h_1 = h_2$ and the ice is completely melted.

## 5. Heat source in a cold environment

We now briefly consider a variation of the above method, where an ice layer in a cold environment is heated from below. This example is motivated by de-icing systems, see [21,25] for example.

Initially we will assume that the ice is in a steady-state, determined by the ambient conditions. Energy is then applied to the lower surface; this represents switching on a de-icing device. The initial temperature of the ice is governed by the steady-state heat equation, $\theta_{zz} = 0$, subject to

$$\theta = T_s|_{z=0}, \quad \theta_z = \alpha_3 + \alpha_4(T_a - \theta)|_{z=H}, \tag{54}$$

where $\alpha_3$, $\alpha_4$ depend on the ambient conditions. In the aircraft icing models described in [17,18,20] $\alpha_3 = 1.35 \times 10^5$ C m$^{-1}$, $\alpha_4 = 4.45 \times 10^5$ m$^{-1}$ and $T_s < T_a < T_m$. This gives

$$\theta = \gamma z + T_s, \quad \gamma = \frac{\alpha_3 + \alpha_4(T_a - T_s)}{1 + \alpha_4 H}. \tag{55}$$

Note that with the current values of parameters $\alpha_3, \alpha_4, \gamma > 0$ and so the temperature is greatest at $z = H$. Eq. (55) provides the initial condition. At $t = 0$ a heating system is turned on such that $\theta_z = \alpha_1$ at $z = 0$, where $\alpha_1 < 0$. A typical value for $\alpha_1$ is $\alpha_1 = -1428$ C m$^{-1}$. The temperature near the lower surface starts to rise quickly but near the upper surface the temperature remains the same. Thus we assume that the solution profile is identical to the steady-state solution (55) for some region $\delta_1(t) < z < H$ where $\delta_1(0) = 0$. Then, following the previously described method for melting a block in a warm environment, we assume the temperature in $0 < z < \delta_1(t)$ is of the form

$$\theta(z,t) = a(t) + b(t)(\delta_1(t) - z) + c(t)(\delta_1(t) - z)^3. \tag{56}$$

At $z = \delta_1$ we require $\theta$ and $\theta_z$ to equal the steady-state solution, i.e.

$$\theta(\delta_1, t) = \gamma\delta_1 + T_s, \quad \theta_z(\delta_1, t) = \gamma. \tag{57}$$

These conditions, together with $\theta_z = \alpha_1$ at $z = 0$, determine the coefficients $a, b, c$ and so (56) becomes

$$\theta(z,t) = \gamma\delta_1(t) + T_s - \gamma(\delta_1(t) - z) + \frac{\gamma - \alpha_1}{3\delta_1(t)^2}(\delta_1(t) - z)^3. \tag{58}$$

To determine $\delta_1(t)$ we integrate the heat equation from $z = 0$ to $z = \delta_1$ and substitute $\theta$ from (58). This leads to the simple ODE

$$\delta\frac{d\delta}{dt} = 6\kappa_i, \tag{59}$$

which is independent of $\alpha_1$. Applying $\delta_1(0) = 0$ gives $\delta(t) = \sqrt{12\kappa_i t}$. So the boundary layer thickness only depends on the thermal diffusivity and time. This solution is valid before melting begins, i.e. while $\theta(0,t) < T_m$. The boundary layer thickness when melting starts is found from (58) by setting $\theta(0, t_1) = T_m$. The time is then

$$t_1 = \frac{3(T_s - T_m)^2}{4\kappa_i(\alpha_1 - \gamma)^2}. \tag{60}$$

Since the external parameters, represented by $T_m$, $T_s$ and $\gamma$, are fixed, this equation indicates the appropriate energy input $\alpha_1$, required to cause melting within a specified time. It is interesting to note that the ambient temperature $T_a$ does not appear in (60). This is because, in this example, the boundary layer does not extend through the ice. As soon as $\delta_1 = H$ we have to change the boundary conditions on $\theta$ and then $T_a$ will play a role.

Fig. 9 shows temperature profiles before melting begins. The parameter values used are $\alpha_1 = -1428$ C m$^{-1}$, $\alpha_3 = 1.35 \times 10^5$ C m$^{-1}$, $\alpha_4 = 4.45 \times 10^5$ m$^{-1}$, $T_s = -10$ °C, $T_a = -8$ °C and $H = 0.023$ m; all other parameter values are taken from Tables 1 and 2. The dashed line denotes the initial condition (55) and the other lines denote the temperature at $t = 7, 14, 21, t_1$s. The final time, $t_1 = 27.695$ s, is found using (60). It can be seen that this profile has $\theta(0, t_1) = 0$. The position of $\delta_1$ is marked by a '*'.

In general, when considering de-icing, it is not sufficient to simply calculate up to the time at which melting first occurs. The ice is typically still frozen at some other point and a water layer may grow for a short time until the aerodynamic forces cause the ice to break off. Consequently we may also need to know about the evolution after melting. We therefore introduce the water temperature $T$ and interface position $h_1(t)$, for $t \geqslant t_1$ and $h_1(t_1) = 0$. Using the method described in Section 3.1 we approximate the solution of the heat equation in the water by re-scaling using

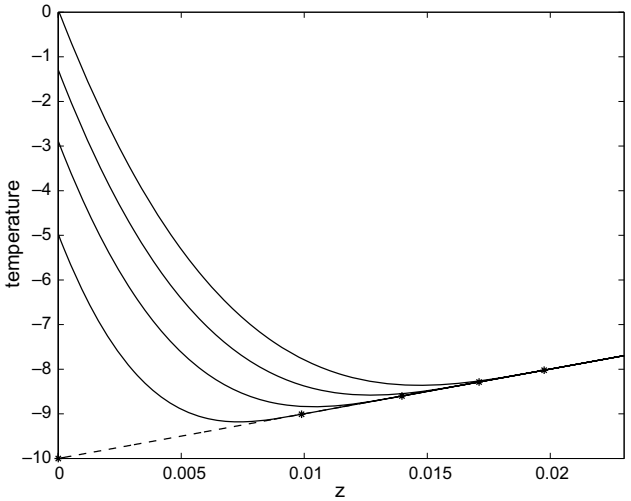


Fig. 9. Solution profiles of the aircraft icing example before melting begins, at $t = 0$ (dashed line) and $t = 7$, 14, 21, 27.6951 s (solid lines).

(15) and considering a series expansion in terms of the small parameter $\epsilon$. Here the boundary conditions are $T_z = \alpha_5 (= k_i \alpha_1 / k_w)$ at $z = 0$, for some $\alpha_5 < 0$, and $T = T_m$ at $z = h$. The solution up to $\mathcal{O}(\epsilon)$ is given by

$$T = T_m - \alpha_5 (h_1 - z) + \frac{\alpha_5}{2\kappa_w} (h_1^2 - z^2) \frac{dh_1}{dt}. \tag{61}$$

In the ice the temperature is given by

$$\theta = \gamma \delta_1(t) + T_s - \gamma(\delta_1(t) - z) + \frac{\gamma h_1 + T_s - T_m}{(h_1(t) - \delta_1(t))^3} (\delta_1(t) - z)^3 \tag{62}$$

for $h_1(t) < z < \delta_1(t)$. For $\delta_1(t) < z < H$ the steady-state solution (55) holds provided $\delta_1 \leqslant h_1$. Using (61) and (62) in the Stefan condition we can then follow the evolution of the film height until $\delta_1 = H$, at which point it would be necessary to switch to a different model. However, we stop the calculation here since the general idea is as specified in the previous section and also because it is not necessary to calculate a thick water film for this application.

## 6. Conclusions

In this paper we have developed an approximate solution method to describe one-dimensional melting from an initial heating phase until completion of the melting process. In the solid phase we employed a modification of the heat balance integral method. Our approximation proved to be significantly more accurate in certain cases and of a similar accuracy in the cases where the approximation of Goodman and Shea held. Furthermore, the cubic approximation is consistent with the expansions of the analytical solutions when such solutions are available. In the water layer an asymptotic analysis also led to a cubic approximation.

The method involves a number of different phases which complicate the solution. However, the same would be true of a numerical solution, as the number of domains and moving boundaries increases. This semi-analytical method then has the advantage that the dependence of the solution on the ambient conditions may be provided explicitly.

The analysis presented here focussed on two examples. In the first a solid block was placed on a warm substrate in a warm environment and the melting followed through its various phases. This example highlighted the different stages and how they progress. Of course there are other possible scenarios but these will all follow similar lines to this example. In our second example we dealt with the problem of heating an ice layer from below. This relatively simple analysis provides an analytical formula which may be used to determine the amount of energy required to melt the base in a given time, or equivalently the time taken for melting to start with a given energy source. This has a clear application in the development of de-icing equipment.

## Acknowledgements

TM acknowledges the support of the Korean Advanced Institute of Science and Technology where a large part of this work was carried out. GM acknowledges the support of the Canon-Collins Trust, SM acknowledges the University of Cape Town Post-Doctoral Fellowship.

## References

[1] T.W. Brakel, J.P.F. Charpin, T.G. Myers, One-dimensional ice growth due to incoming supercooled droplets impacting on a thin conducting substrate, Int. J. Heat Mass Transfer 50 (2007) 1694–1705.
[2] J. Caldwell, C.C. Chan, Numerical solution of Stefan problems in annuli by enthalpy method and heat balance integral method, Comm. Numer. Methods Eng. 17 (6) (2001) 395–405.
[3] J. Caldwell, C.K. Chiu, Numerical solution of one-phase Stefan problems by the heat balance integral method, Part I – Cylindrical and spherical geometries, Comm. Numer. Methods Eng. 16 (8) (2000) 569–583.
[4] H.S. Carslaw, J.C. Jaeger, Conduction of Heat in Solids, second ed., Clarendon Press, 1959.
[5] S.J. Citron, Heat conduction in a melting slab, J. Aero. Sci. (1960) 219–228.
[6] J. Crank, Mathematics of Diffusion, Clarendon Press, Oxford, 1975.
[7] R.W. Gent, N.P. Dart, J.T. Cansdale, Aircraft icing, Philos. Trans. R. Soc. Lond. A 358 (1776) (2000) 2873–2911.
[8] T.R. Goodman, The heat-balance integral and its application to problems involving a change of phase, Trans. ASME 80 (1958) 335–342.
[9] T.R. Goodman, J.J. Shea, The melting of finite slabs, J. Appl. Mech. 27 (1960) 16–27.
[10] J.M. Hill, One-Dimensional Stefan Problems: An Introduction, Longman Sci. Tech., Harlow, 1987.
[11] E. Javierre, C. Vuik, F.J. Vermolen, S. van der Zwaag, A comparison of numerical models for one-dimensional Stefan problems, J. Comput. Appl. Math. 192 (2006) 445–459.
[12] J.L. Laforte, M.A. Allaire, J. Laflamme, State of the art on power line de-icing, Atmos. Res. 46 (1998) 143–158.
[13] H.G. Landau, Heat conduction in a melting solid, Quart. Appl. Math. 8 (1950) 81–94.
[14] F. Mosally, A.S. Wood, A. Al-Fhaid, An exponential heat balance integral method, Appl. Math. Comput. 130 (2002) 87–100.
[15] F. Mosally, A.S. Wood, A. Al-Fhaid, On the convergence of the heat balance integral method, Appl. Math. Modell. 29 (2005) 903–912.
[16] T.G. Myers, Extension to the Messinger Model for aircraft icing, AIAA 39 (2001) 211–218.
[17] T.G. Myers, J.P.F. Charpin, A mathematical model for atmospheric ice accretion and water flow on a cold surface, Int. J. Heat Mass Trans. 47 (2004) 5483–5500.
[18] T.G. Myers, J.P.F. Charpin, S.J. Chapman, The flow and solidification of a thin fluid film on an arbitrary three-dimensional surface, Phys. Fluids 14 (2002) 2788–2803.
[19] T.G. Myers, J.P.F. Charpin, C.P. Thompson, Slowly accreting ice due to supercooled water impacting on a cold surface, Phys. Fluids 14 (2002) 240–256.
[20] T.G. Myers, D.W. Hammond, Ice and water film growth from incoming supercooled water droplets, Int. J. Heat Mass Transfer 42 (1999) 2233–2242.
[21] G.I. Poots, Ice and Snow Accretion on Structures, Springer, UK, 1996.
[22] N. Popov, S. Tabakova, F. Feuillebois, Numerical modelling of the one-phase Stefan problem by finite volume method, Numerical Analysis and Its Applications, vol. 3401, Springer, Berlin/Heidelberg, 2005, pp. 456–462.

[23] H. Schlichting, Boundary Layer Theory, eighth ed., Springer, 2000.
[24] T.J. Sheer, Pneumatic conveying of ice particles through mine-shaft pipelines, Powder Technol. 85 (1995) 203–219.
[25] S.K. Thomas, R.P. Cassoni, C.D. MacArthur, Aircraft anti-icing and de-icing techniques and modelling, J. Aircraft 33 (5) (1996) 841–854.
[26] S.K. Wong, A. Walton, Numerical solution of single-phase Stefan problem using a fictitious material, Numer. Heat Transfer, Part B 35 (1999) 211–223.
[27] A.S. Wood, A new look at the heat balance integral method, Appl. Math. Modell. 25 (2001) 815–824.
[28] M. Zerroukat, C.R. Chatwin, An explicit unconditionally stable variable time-step method for one-dimensional Stefan problems, Int. J. Numer. Methods Eng. 35 (1992) 1503–1520.